Bioplastic biodegradability shapes microbial communities in a coastal brackish environment

Igor S. Pessi[1,2,3,#,†], Eeva Eronen-Rasimus[1,2,#], Pinja Näkki[1], David N. Thomas[4,3], and Hermanni Kaartokallio[1]

[1]Marine and Freshwater Unit, Finnish Environment Institute (Syke), Helsinki, Finland
[2]Department of Microbiology, University of Helsinki, Helsinki, Finland
[3]Helsinki Institute of Sustainability Science (HELSUS), Helsinki, Finland
[4]Department of Environmental Sciences, University of Helsinki, Helsinki, Finland
[#]Both authors contributed equally to this work
[†]Corresponding author: igor.pessi@gmail.com

Igor S. Pessi: https://orcid.org/0000-0001-5926-7496
Eeva Eronen-Rasimus: https://orcid.org/0000-0002-1749-0793
Pinja Näkki: https://orcid.org/0000-0003-2499-4751
David N. Thomas: https://orcid.org/0000-0001-8832-5907
Hermanni Kaartokallio: https://orcid.org/0000-0002-3650-4628

Abstract

Microorganisms are metabolically versatile and central to marine ecosystems, yet the potential of marine microbial communities to degrade different bioplastics and the effect of environmental factors are poorly understood. Employing multi-seasonal *in situ* and *in vitro* experiments, we assessed the biodegradation of six commonly used bio-based bioplastic materials at a coastal site in the brackish Baltic Sea and characterised the associated microbial communities using metagenomics and metatranscriptomics. Cellulose acetate (CA), polybutylene succinate (PBS), and polyhydroxybutyrate/valerate (PHB) degraded at varying rates across materials, seasons, and experimental settings, with up to 28% weight attrition after 97 weeks *in situ* (CA) and 56% carbon loss to CO_2 after four weeks *in vitro* (PBS). The three biodegraded plastics developed similar microbial communities that differed markedly from those on the other materials (cellulose acetate propionate, polyamide, and polyethylene) and in the water column. The main microbial populations on the biodegraded plastics included aerobic and facultative anaerobic heterotrophs with a broad capacity for carbohydrate metabolism. Populations with the potential for nitrogen fixation and denitrification were more prevalent on the biodegraded plastics, suggesting a link with the marine nitrogen cycle. Based on the metatranscriptomic signal of key genes involved in the initial hydrolysis of CA, PBS, and PHB, we identified diverse microbial populations that can potentially drive the biodegradation of these materials in the Baltic Sea, many of which encoded the potential to degrade multiple bioplastics. We propose the term *bioplastisphere* to denote the distinctive microbial communities associated with biodegradable plastics.

Introduction

Millions of tonnes of plastics enter the oceans annually, making plastic pollution one of the most pervasive environmental challenges of our time [1–3]. Plastics accumulate in coastal regions, surface waters, and sediments, where they can cause long-lasting environmental harm [4–6]. The amount of mismanaged plastic waste in the environment is projected to triple in the coming decades due to increasing industrial and societal demands combined with inadequate waste management practices [7]. Conventional fossil fuel-based plastics, particularly polyethylene, dominate the plastic industry due to their high durability against biotic and abiotic processes, which also makes them the main constituents of marine plastic pollution [7, 8]. Bioplastics—*i.e.* plastics that are biodegradable or produced from renewable, bio-based sources—have become increasingly popular as part of a wider strategy to reduce environmental pollution and the use of finite fossil fuel resources [9]. However, many bioplastic materials only achieve full biodegradation under tightly constrained conditions, such as those certified by the EU standard EN13432 for industrial composting [10]. Plastic biodegradation is much slower in marine environments, which are generally colder, more oligotrophic, and contain lower microbial biomass and diversity than compost and soil [11]. Because both material properties and environmental conditions influence plastic biodegradation, there is little consensus about the general biodegradability of different bioplastic materials [12, 13]. Current industrial directives do not address adequately the impacts of mismanaged bioplastic waste in marine environments, which remain poorly understood.

Plastics can serve as substrate for microbial growth and biofilm formation in marine environments, and microorganisms are the main drivers of plastic biodegradation [14–16]. Microorganisms colonise marine plastics readily and communities are considered mature in the order of one month [17–20]. Communities associated with plastic debris, which are collectively known as the plastisphere, are generally dominated by *Alpha-* and *Gammaproteobacteria* and include potentially hydrocarbonoclastic genera [21–24]. In certain biodegradable plastics, the abundance of *Alpha-* and *Gammaproteobacteria* has been associated with the loss of substrate or observed biodegradation [18, 25, 26]. Plastisphere communities are mostly shaped by biogeographical and environmental factors [21, 22, 27–29], and the importance of material properties is under debate [19, 22, 23, 29, 30]. Communities growing on conventional plastics are usually similar to those on totally inert surfaces (*e.g.* glass) and are characterised by a secondary biofilm community that is not in close contact with the substrate, with differences in community composition mostly driven by rare taxa [19, 22]. Conversely, increasing evidence suggests that microbial communities colonising some bioplastic materials (*e.g.* polyhydroxybutyrate and cellulose acetate) are different and more active than those on conventional plastics, whereas communities on bioplastics that have limited biodegradation in marine environments (*e.g.* polylactic acid) resemble those on conventional plastics [18, 24–26, 31, 32]. Recent studies have shown that metagenomics is a powerful tool to investigate the functional potential of microbial communities and their role not only in plastic biodegradation but also other biogeochemical

processes. For example, increased denitrification potential as communities mature during the first months of plastic colonization has been observed in a coastal estuary [24]. This study also showed that genes for nitrogen metabolism are typically present in many common plastisphere taxa such as *Alpha-* (*e.g. Rhizobiales* and *Rhodobacterales*) and *Gammaproteobacteria* (*e.g. Burkholderiales* and *Pseudomonadales*).

Key to a better understanding of the impact of marine plastics on marine environments is to consider biodegradation as a systemic capacity, *i.e.* by investigating the associated microbial communities and the environmental conditions constraining their activity. However, long-term *in situ* investigations are rare, particularly studies of bioplastic biodegradation coupled with the analysis of microbial communities [19, 26, 32–37]. Data on community composition and activity at the functional level are also scarce, including not only the microbial pathways of bioplastic biodegradation but also their connections with the marine carbon and nitrogen cycles. In this study we assessed the biodegradation of six commonly used bio-based bioplastic materials at a coastal site in the brackish Baltic Sea under multi-seasonal *in situ* and *in vitro* conditions. Coupling measurements of plastic weight attrition, spectroscopy, respirometry, metagenomics, and metatranscriptomics, we investigated differences in biodegradation between the materials throughout different seasons and explored links between biodegradation and microbial community structure and activity. We hypothesised that the composition of mature (> 1 month) communities—including the presence and activity of plastic-degrading genes—is structured by the physicochemical properties of the bioplastics and therefore unique to each material.

Materials and Methods

Experimental setup

Bioplastic materials. We investigated six types of bio-based bioplastics, which will be designated as bioplastics: cellulose acetate (CA), cellulose acetate propionate (CAP), polybutylene succinate (PBS), polyhydroxybutyrate/valerate (PHB), polyamide (PA), and polyethylene (PE). The materials were selected to represent a range of commonly used bioplastics with distinct molecular structures and included *i*) natural polymers with known marine biodegradability (CA and PHB); *ii*) bio-based polymers with unclear marine biodegradability (PBS, CAP, and PA); and *iii*) non-biodegradable polymers (PE). Injection-moulded bioplastic sheets were provided by the VTT Technical Research Centre of Finland (Espoo, Finland).

***In situ* mesocosm.** *In situ* biodegradation was investigated for 97 weeks in a mesocosm experiment set up at the Tvärminne Zoological Station, University of Helsinki (Hanko, Finland, 59.845°N, 23.250°E). The salinity of the seawater at the study site is between 5 and 6 and the water temperature during the experiment ranged from 2.5°C to 25.0ºC. In July 2021, 60 bioplastic sheets (15 mm width × 100 mm length × 3 mm thick) of each material were weighed using an EP-225-SM-DR semi-micro balance (Precisa Gravimetrics, Dietikon, Switzerland), secured to racks, and transferred to a 400 l flow-through tank connected to the

118 Baltic Sea. Glass sheets of identical dimensions were included as control. The mesocosm was
119 kept in the dark to prevent the growth of photosynthetic microeukaryotes. At six sampling
120 times (September 2021, January, March, and August 2022, and January and May 2023), five
121 sheets of each material were sampled for measuring biodegradation and five for
122 metagenomics and metatranscriptomics. Five seawater samples (1000 ml) were also taken
123 from inside the mesocosm tank for the molecular characterization of the planktonic
124 communities. The samples for measuring biodegradation were kept at –20°C until processing
125 and the other samples were processed immediately.

126 ***In vitro* experiments.** For the seven sampling times indicated above (July 2021–May 2023)
127 and each bioplastic material (except CAP, which was not included due to equipment
128 availability), 0.25 g l^{-1} of finely milled bioplastic (< 0.3 mm particle size) was added to three
129 600 ml amber-coloured bottles containing 250 ml of seawater sampled from the mesocosm
130 tank. To prevent nutrient limitation, 0.1 g l^{-1} KH_2PO_4 and 0.5 g l^{-1} NH_4Cl were added.
131 Microcrystalline cellulose with an average particle size of 90 µm (Xylem Analytics, Weilheim,
132 Germany) was used as positive control, and negative controls without bioplastic were also
133 included. The bottles were incubated with agitation in the dark at 15°C for 28 days and then
134 processed immediately.

135 Biodegradation measurements

136 *In situ* biodegradation was estimated based on the weight attrition of the bioplastic sheets.
137 The sheets were immersed in 2% sodium dodecyl sulfate and incubated overnight at 35°C
138 with mild agitation, then brushed gently, rinsed with ultrapure water, and dried overnight
139 at room temperature. The sheets were then weighed using a semi-micro balance (EP-225-
140 SM-DR), and the weight attrition was calculated as the difference between the initial and
141 post-incubation weights divided by the initial weight. Changes in the surface chemical
142 structure of the bioplastic sheets were assessed using an Agilent 4300 Fourier transform
143 infrared (FTIR) spectrometer (Agilent, Santa Clara, USA) in the spectral range of 650–4000
144 cm^{-1}. The spectra were compared to reference data from the Polymers and Polymer Additives
145 Spectra Database P/N 30002 with *MicroLab* v5.8 [38]. *In vitro* bioplastic biodegradation was
146 estimated according to the D6691-17 standard [39] using a WTW OxiTop-IDS12 respirometer
147 (Xylem Analytics, Weilheim, Germany), which records biological oxygen demand (BOD) by
148 pressure difference from the absorption of CO_2 evolved during incubation with NaOH. BOD
149 was converted to carbon loss to CO_2 based on carbon contents determined using a CHN
150 analyser (ALS, Prague, Czechia).

151 Metagenome and metatranscriptome sequencing

152 The *in situ* bioplastic sheets were scraped using a sterile scalpel and the biofilms were
153 transferred to 2 ml Lysing Matrix E tubes (MP Biomedicals, Irvine, USA). The *in situ*
154 seawater and the *in vitro* samples were vacuum filtered through Whatman 0.22 µm
155 membrane filters (Cytiva, Marlborough, USA) and transferred to 2 ml cryovials. The tubes
156 were flash-frozen in liquid nitrogen and stored at –80°C. DNA and RNA were co-extracted
157 using a modified cetrimonium bromide (CTAB), phenol-chloroform, and bead-beating protocol

158 [40]. After bead-beating, the extract was transferred to a clean tube and centrifuged at 16,000
159 × g for 5 min at 4°C. The top aqueous layer was transferred to a clean tube containing 500 µl
160 of ≥ 99.9% stabilised chlorophorm (VWR Chemicals, Radnor, USA), and the extraction
161 continued as further described [40]. Blank samples were extracted and sequenced in parallel.
162 Library preparation and sequencing were done at the DNA Sequencing and Genomics
163 Laboratory (University of Helsinki, Helsinki, Finland). The DNAprep kit (Illumina, San
164 Diego, USA) with in-house Nextera primers was used for metagenomics and the NEBNext
165 Ultra II Directional RNA kit (New England Biolabs, Ipswich, USA) for metatranscriptomics.
166 The libraries were sequenced using the NovaSeq 6000 system (Illumina) and the S4
167 chemistry (2 × 150bp). In total, 391 metagenomes and 78 metatranscriptomes were
168 sequenced, yielding 1.5 Tb and 508.6 Gb with a median output of 3.6 Gbp and 7.0 Gbp per
169 sample, respectively (**Table S1**). Some PA, PE, and glass metagenomes and
170 metatranscriptomes yielded few reads, and several metatranscriptomes could not be
171 sequenced due to low RNA yield.

172 ## Taxonomic profiling

173 *Cutadapt* v4.4 [41] was used to trim sequencing adapters, low quality base calls (Phred score
174 < 28), and poly-A tails, and to discard short reads (< 50 bp after trimming) and reads
175 containing ambiguous base calls. The quality of the raw and filtered data was assessed with
176 *FastQC* v0.12.1 [42] and *MultiQC* v1.15 [43]. The filtered metagenomic and
177 metatranscriptomic reads were classified at the domain level using *Kaiju* v1.10.0 and the
178 *nr_euk* database release 2023-05-10 [44]. A more detailed taxonomic profiling of bacteria and
179 archaea was obtained based on 59 single-copy marker genes with *SingleM* v0.16.0 [45] and
180 the genome taxonomy database (GTDB) release 214 [46]. A consensus taxonomic profile was
181 obtained by summarizing the coverage of each taxon across the 59 marker genes.

182 ## Metagenome assembling and binning

183 The metagenomes were assembled and binned using the *snakemake* metagenomics workflow
184 in *anvi'o* v7.1 [47]. For each group of 3 or 5 replicates (*in vitro* an *in situ* incubations,
185 respectively), the filtered reads were pooled and assembled using *MEGAHIT* v1.2.9 [48] with
186 a minimum contig length of 1000 bp, and gene calls were identified with *Prodigal* v2.6.3 [49].
187 Taxonomy was assigned to the contigs based on a set of 71 bacterial and 76 archaeal single-
188 copy genes [50] identified with *HMMER* v.3.3.2 [51] and classified with *DIAMOND* v2.1.7
189 [52] against the GTDB release 89 [46]. The metagenomic reads were mapped to the contigs
190 with *Bowtie2* v2.3.5 [53] and *SAMtools* v1.10 [54], and *MetaBAT2* v2.15 [55] was used to bin
191 metagenome-assembled genomes (MAGs) based on tetranucleotide frequency and differential
192 coverage. The MAGs from the different assemblies were pooled and pairwise average
193 nucleotide identity (ANI) values were computed with *FastANI* v1.3.2 [56]. For each cluster of
194 MAGs representing closely related populations with ≥ 98% ANI, a representative MAG with
195 the highest score was selected, where

196 $$score = completion - 2 \times redundancy + 0.5 \times \log(N_{50}) + 0.5 \times \log(length) \text{ (modified from [57]).}$$

197 The non-redundant MAGs were visually inspected with *anvi'o* v8.0 [47] and the contigs with
198 discrepant coverage, tetranucleotide frequency, or taxonomic signal were removed [58]. The
199 MAGs were classified against the GTDB release 214 [46] with *GTDB-Tk* v2.3.0 [59]. The
200 metagenomic and metatranscriptomic reads were mapped to the curated MAGs with *Bowtie2*
201 v2.5.1 [53] and *SAMtools* v1.18 [54], and *CoverM* v0.7.0 [60] was used to count the number of
202 reads recruited by each MAG applying the reads per kilobase per million mapped reads
203 (RPKM) transformation. Only matching reads with ≥ 95% sequence identity and ≥ 75%
204 coverage and MAG-level horizontal coverage/detection ≥ 25% were considered to limit the
205 effect of non-specific mapping.

206 Annotation of metabolic and plastic-degrading genes

207 MAG-level metabolic traits were reconstructed with *microTrait* v1.0.0 [61] and the
208 prevalence of each trait was calculated as the proportion of MAGs containing the trait
209 relative to all the MAGs detected in a given sample. Putative plastic-degrading genes were
210 searched against the CAZy database [62] with *HMMER* v.3.3.2 [51] (CA; e-value < 10^{-12}) and
211 the PlasticDB database [63] with *DIAMOND* v2.1.8 [52] (PBS and PHB; ≥ 30% amino acid
212 similarity and ≥ 70% alignment). Relatively low thresholds were applied initially to capture
213 potentially distant homologs. For each putative plastic-degrading gene, the coverage in the
214 corresponding *in vitro* metatranscriptomes was extracted with *anvi'o* v8.0 [47], and genes
215 with mean horizontal coverage ≥ 25% were considered active.

216 Statistical analyses

217 Statistical analyses were done in *R* v4.3.3 [64]. Microbial richness and beta-diversity were
218 computed based on the read count of unique variants of the *rpsB* gene, which is a single-copy
219 housekeeping gene encoding the universal ribosomal protein S2 of bacteria and archaea.
220 Samples with < 325 *rpsB* reads (the median value across the dataset) were discarded in both
221 analyses and microbial richness was estimated after subsampling the dataset. Significant
222 differences in biodegradation and microbial richness between the materials were assessed
223 using analysis of variance (ANOVA) followed by the Sidak test using the packages *stats* v4.3.3
224 [64], *emmeans* v1.10.6 [65], and *multcomp* v1.4.26 [66]. For beta-diversity analyses, the *rpsB*
225 counts were standardised using the Hellinger transformation, pairwise Bray-Curtis
226 dissimilarities were computed, and differences in community structure were assessed by
227 principal coordinates analysis (PCoA) and permutational multivariate ANOVA
228 (PERMANOVA) using the package *vegan* v2.7.1 [67]. Differentially abundant genera, traits,
229 and MAGs were identified using linear regression with the package *Maaslin2* v1.16.0 [68].
230 The data were log-transformed prior to model fitting, and the *P* values were adjusted using
231 the Benjamini-Hochberg false discovery rate (FDR). Observations with adjusted $P < 0.05$ and
232 log2 fold change (log2FC) ≥ 3 were considered differentially abundant, the latter
233 corresponding to a ≥ 8-fold difference between the treatments.

Results

In situ and *in vitro* bioplastic biodegradation

Biofilms were visible on the CA, PBS, and PHB sheets 12 weeks after the start of the *in situ* mesocosm experiment (**Fig. 1a**). CA and PBS, in particular, developed thick, slimy biofilms with pronounced black pigmentation. Biofilms were less developed on the other bioplastic materials (CAP, PA, and PE) and the control surface (glass). *In situ* biodegradation rates based on weight attrition differed between the bioplastic materials (ANOVA, $R^2 = 0.99$, $P < 0.001$) (**Fig. 1b**). CA degraded the most (27.8% ± 0.2% weight attrition after 97 weeks) followed by PBS (12.7% ± 1.0%) and PHB (7.1% ± 0.2%). Weight attrition was negligible for CAP (1.3% ± 0.2%) and below detection for PA and PE. A comparable pattern was observed using FTIR spectroscopy, which revealed changes in the surface chemical structure of the CA, PBS, and PHB sheets but not CAP, PA, and PE (**Fig. 1c**).

I*n vitro* biodegradation rates based on respirometry also varied between the materials (ANOVA, $R^2 = 0.71$, $P < 0.001$) (**Fig. S1**). PBS degraded the most (56.0% ± 7.2% carbon loss to CO_2 after four weeks) followed by CA (32.8% ± 2.2%) and PHB (26.8% ± 11.5%). Negligible

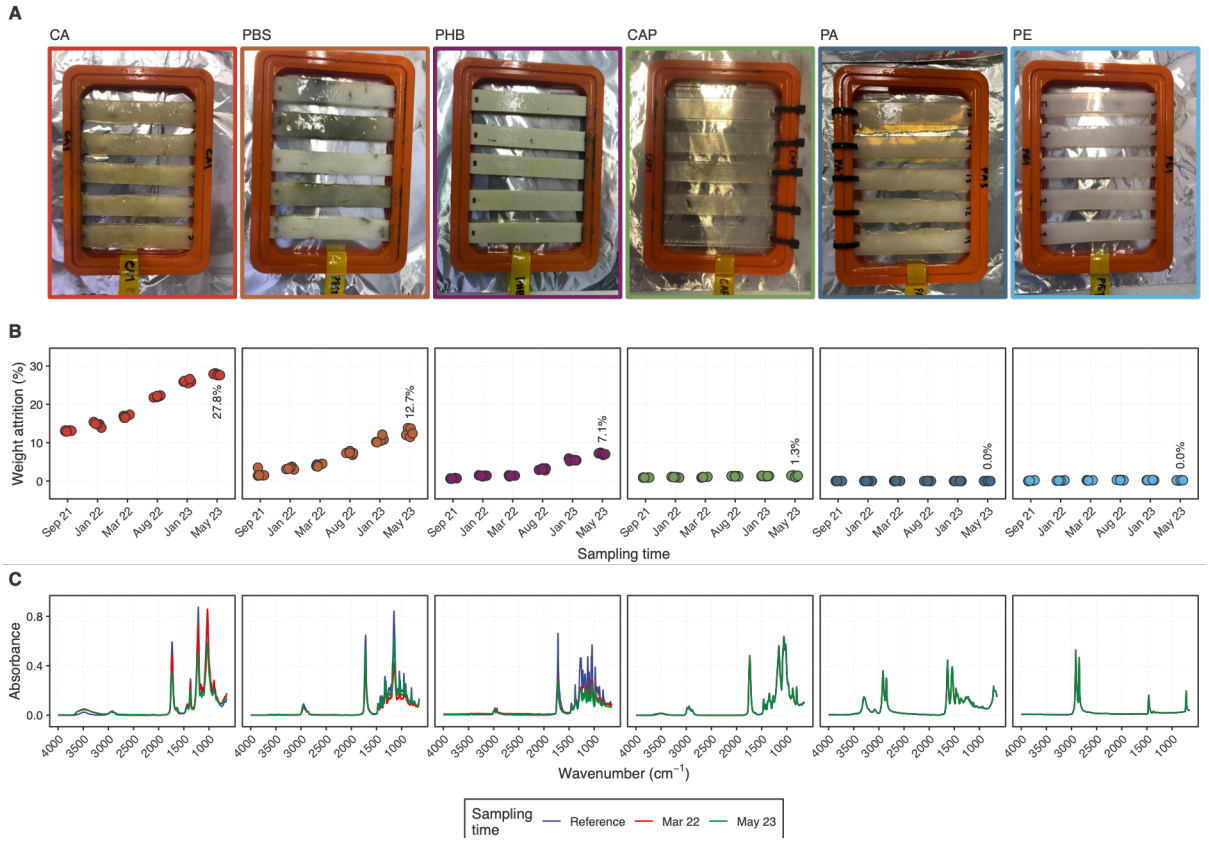

Figure 1. Biodegradation of six bio-based bioplastic materials in a 97-week *in situ* mesocosm experiment in the Baltic Sea. a) Pictures of the bioplastic sheets after 12 weeks (September 2021). **b)** Biodegradation rates based on weight attrition relative to the start of the experiment (July 2021). **c)** Fourier transform infrared spectra of the bioplastic sheets after 38 and 97 weeks (March 2022 and May 2023, respectively).

249 carbon loss was measured for PA and PE (1.8% ± 1.4% and 1.1% ± 1.0%, respectively), likely
250 reflecting the utilisation of residual plastic additives. The *in vitro* biodegradation of CAP was
251 not assessed. Temporal differences in biodegradation were observed for some materials
252 (ANOVA, R^2 = 0.95–0.99, P < 0.001). Whereas CA degraded uniformly, PBS varied from 7.0
253 ± 0.0% to 62.7% ± 4.7% and PHB from 10.7% ± 0.6% to 44.3% ± 5.0%. PBS and PHB had the
254 highest biodegradation for communities sampled in winter (January 2022 and 2023,
255 respectively).

256 Microbial communities associated with the bioplastics

257 In line with our hypothesis, the analysis of reads matching the *rpsB* gene showed that the
258 metagenomes were structured by material (PERMANOVA, R^2 = 0.26, P < 0.001). The PCoA
259 further clustered the metagenomes into four groups comprising *i)* the three biodegraded
260 plastics (CA, PBS, and PHB); *ii*) the slowly degrading bioplastic (CAP); *iii*) the inert surfaces,
261 including the bioplastics that did not degrade (PA and PE) and the control material (glass);
262 and *iv*) the planktonic seawater metagenomes (**Fig. 2a**). The metagenomes from the
263 biodegraded plastics and CAP had lower microbial richness than the other two groups
264 (ANOVA, R^2 = 0.63, P < 0.001) (**Fig. 2b**). The metagenomes were also temporally structured
265 (PERMANOVA, R^2 = 0.09–0.22, p < 0.001) (**Fig. S2**). The temporal dynamics varied between
266 the biofilm and planktic datasets, with the biofilm metagenomes from both the biodegraded
267 and non-biodegraded plastics diverging linearly over time, whereas the planktic seawater
268 metagenomes followed a seasonal dynamic. The PHB metagenomes from January 2023 were
269 markedly distinct from the other sampling times. Consistent microbial structure was
270 observed for the biodegraded plastics across the *in situ* and *in vitro* metagenomes and
271 metatranscriptomes (**Fig. S3**), which suggests that we were able to capture an active
272 microbial community that is likely linked to the biodegradation of these materials. In
273 contrast, the *in situ* PA and PE metagenomes clustered with the glass metagenomes, whereas
274 the *in vitro* PA and PE metagenomes were similar to the seawater metagenomes and
275 metatranscriptomes, suggesting activity not related to the substrate.

276 Potential microbial drivers of bioplastic biodegradation

277 Comparison with sequences from the GenBank *nr* database revealed that bacteria comprised
278 a large fraction (98.0% ± 0.2% of the reads) of the *in situ* and *in vitro* metagenomes (**Fig. S4**).
279 Both experiments were done in the dark to target heterotrophs and so the metagenomes
280 contained very few reads assigned to photosynthetic microeukaryotes, which are usually
281 abundant members of the plastisphere [30, 69]. More detailed analysis of the bacterial
282 community based on single-copy marker genes showed that the bioplastic metagenomes were
283 dominated by members of the *Gamma-* (26.8% ± 1.2% of the reads) and *Alphaproteobacteria*
284 (22.6% ± 0.6%), followed by *Planctomycetota* (9.6% ± 0.4%), *Actinomycetota* (8.9% ± 0.7%),
285 *Bacteroidota* (5.2% ± 0.2%), *Myxococcota* (2.8% ± 0.2%), *Acidobacteriota* (1.8% ± 0.1%), and
286 *Verrucomicrobiota* (1.3% ± 0.2%) (**Fig. S5**). When considering the abundant genera—defined
287 as those representing ≥ 0.5% of the reads in each material—only a small number of taxa were
288 shared between the biodegraded plastic metagenomes and the other groups, and the three
289 biodegraded plastics collectively contained the largest fraction of the total diversity (**Fig. S6**).

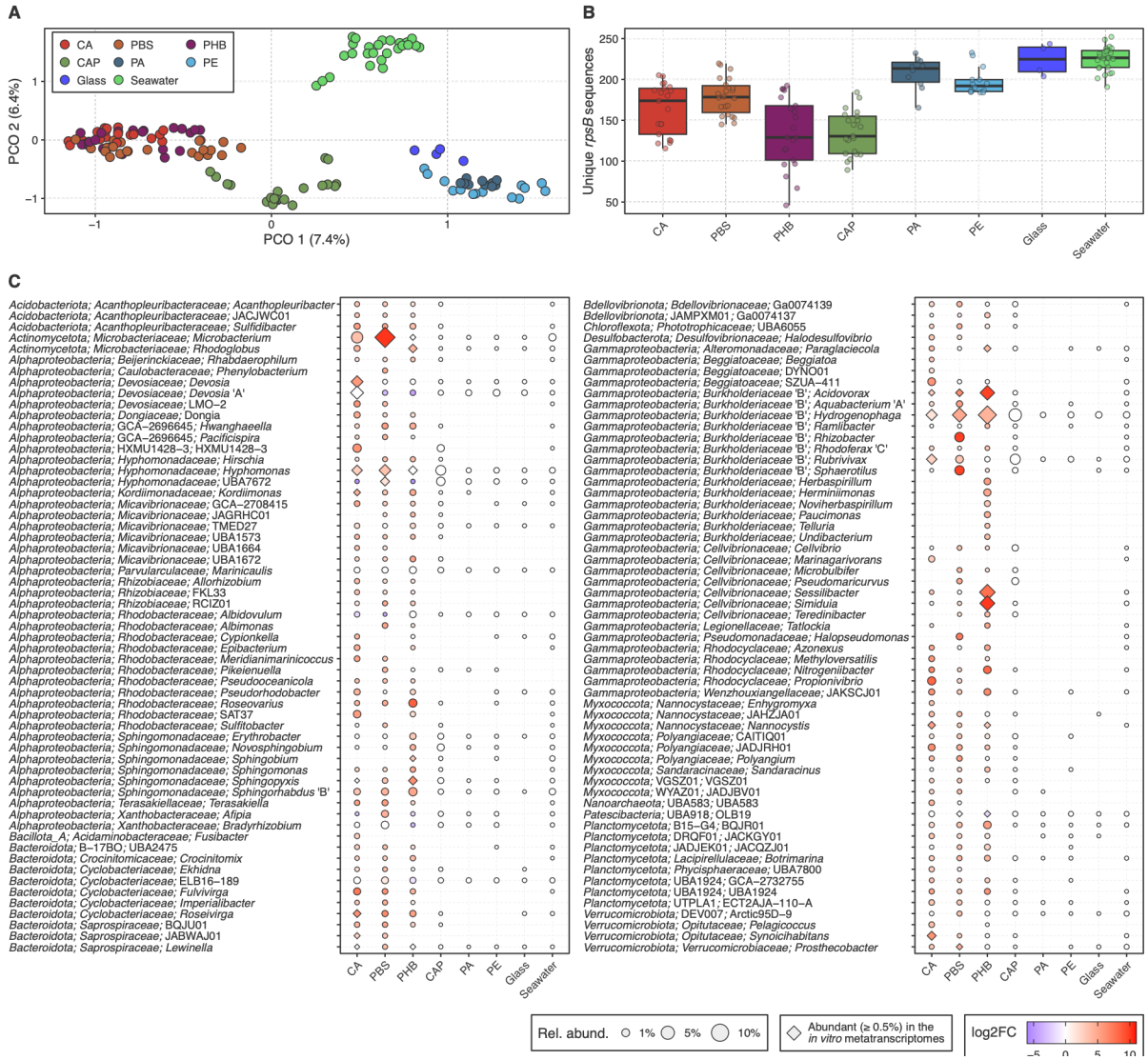

Figure 2. Microbial communities associated with bioplastic degradation in the Baltic Sea. **a)** Microbial community structure based on unique 60-bp *rpsB* sequences extracted from the metagenomic reads. Principal coordinates analysis of Bray-Curtis dissimilarities of Hellinger-transformed counts. **b)** Microbial richness based on unique 60-bp *rpsB* sequences, calculated after subsampling to even depth. In **a** and **b**, samples with < 325 *rpsB* reads were not included. **c)** Distribution of 118 abundant (≥ 0.5%) genera in the biodegraded plastics (CA, PBS, and PHB) and genera that were significantly more abundant in these materials compared to the inert surfaces (PA, PE, and glass) according to linear regression (log2FC ≥ 3.0, adjusted $P < 0.05$). Consensus taxonomic profile based on 59 marker gene sequences extracted from the metagenomic reads. Relative abundance is shown as the 10% trimmed mean across five biological replicates and six sampling times. Genera shown with a diamond were abundant (≥ 0.5%) in the associated *in vitro* metatranscriptomes.

To explore the microorganisms that might be driving bioplastic biodegradation, we considered the abundant genera in the *in situ* CA, PBS, and PHB metagenomes and those that were significantly more abundant in these materials compared to the inert surfaces (linear regression, log2FC ≥ 3.0, adjusted $P < 0.05$). Many genera were shared between the

294 biodegraded plastics, and many were also active in the *in vitro* metatranscriptomes (**Fig. 2c**).
295 For example, *Hydrogenophaga* and *Acidovorax*, both members of the *Gammaproteobacteria*,
296 and *Hyphomonas* (*Alphaproteobacteria*) were among the most abundant and active genera in
297 the metagenomes and metatranscriptomes from the three biodegraded plastics.
298 *Microbacterium* (*Actinomycetota*) was the most abundant genus in the *in situ* PBS and CA
299 metagenomes and was also active in the PBS metatranscriptomes. *Devosia*
300 (*Alphaproteobacteria*) and *Roseivirga* (*Bacteroidota*) were abundant and active in CA, and
301 *Sessilibacter* and *Simiduia* (both *Gammaproteobacteria*) were abundant and active in PHB.

302 ## Microbial traits associated with the bioplastics

303 We assembled and binned the metagenomes to investigate the functional composition of the
304 microbial populations associated with the bioplastics. Binning yielded 5,129 non-redundant
305 MAGs (≥ 98% ANI) which represented a substantial fraction of the metagenomes, recruiting
306 45.4% ± 19.4% of the reads and reaching up to 70% in some samples (**Table S1**). Metabolic
307 reconstruction showed that the functional composition of the *in situ* metagenomes was also
308 structured by material (PERMANOVA, $R^2 = 0.48$, $P < 0.001$), with a clear separation between
309 the biodegraded, non-biodegraded, and seawater metagenomes (**Fig. S7**). Differently to the
310 results based on the *rpsB* gene, the CAP metagenomes clustered with the biodegradable
311 plastics in the functional analysis.

312 We searched the MAGs for key genes involved in the initial hydrolysis of CA, PBS, and PHB
313 to track the microbial populations that are potentially driving the biodegradation of these
314 materials. The prevalence of bioplastic-degrading traits in the *in situ* metagenomes—defined
315 as the proportion of MAGs containing the trait in a sample—was generally higher in the
316 biodegraded plastics compared to the inert surfaces (linear regression, adjusted $P < 0.05$)
317 (**Fig. 3**, **Fig. S8**). Genes encoding carbohydrate esterases (CAZy families CE1 and CE2) and
318 glycoside hydrolases (CAZy families GH5, GH9, GH45, and GH48), which function in CA
319 deacetylation and hydrolysis, respectively, were identified in 11.0% ± 0.4% of the MAGs
320 detected in the biodegradable plastics. Genes functioning in PBS hydrolysis were identified
321 in 11.7% ± 0.3% of the MAGs, and most were related to a PLA depolymerase derived from an
322 uncultured microorganism with verified enzymatic activity against PBS [70]. Finally, genes
323 encoding PHB depolymerases were identified in 40.7% ± 0.6% of the MAGs from the
324 biodegradable plastics, 21.1% ± 2.8% from the inert surfaces and 14.3% ± 0.8 from the
325 seawater metagenomes. Other traits that were more prevalent in the biodegraded plastics
326 included functions related to carbohydrate depolymerization, degradation, and transport, the
327 assimilation and transport of nitrogen, phosphorus, and sulphur compounds, aerobic
328 respiration, anaerobic respiration, pyruvate fermentation, CO_2 fixation, and anoxygenic
329 photosynthesis. In contrast, lithotrophic traits, methane oxidation, and hydrogenotrophic
330 methanogenesis were more prevalent on the inert surfaces (**Fig. 3**, **Fig. S8**).

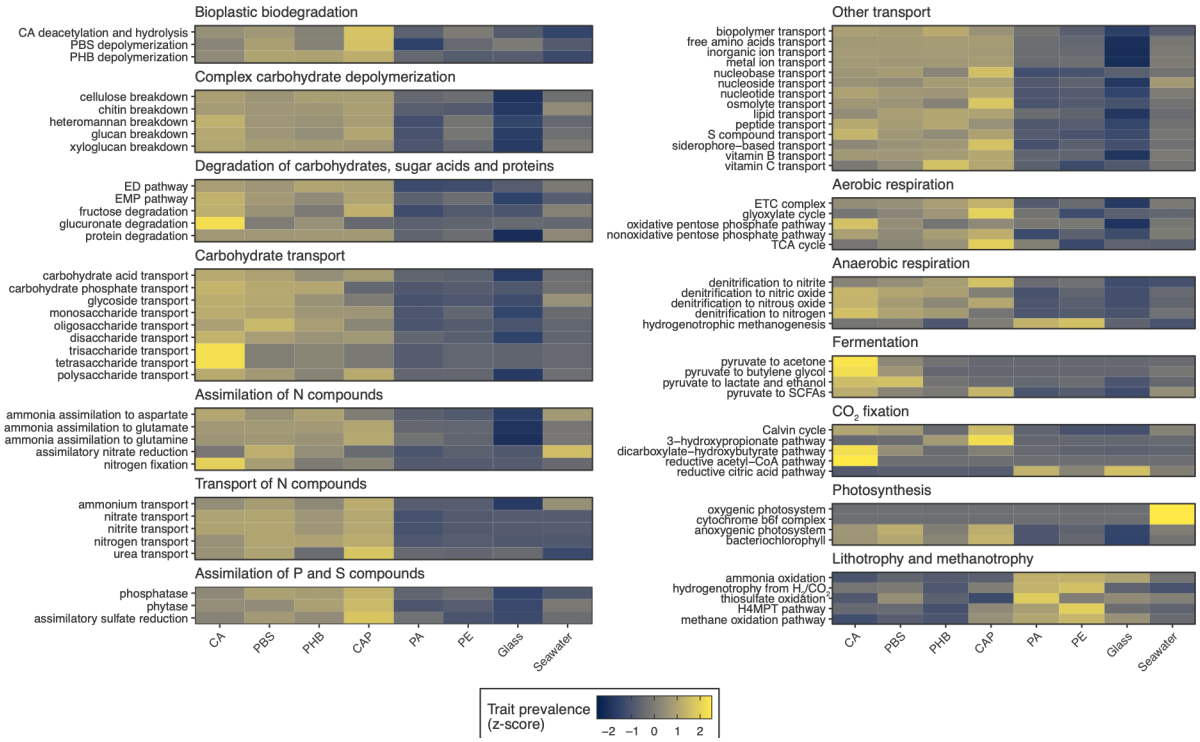

Figure 3. Microbial traits associated with bioplastic biodegradation in the Baltic Sea. Trait prevalence represents the proportion of metagenome-assembled genomes (MAGs) containing the trait relative to all the MAGs detected in a given sample (≥ 25% horizontal coverage). Trait prevalence is shown as the 10% trimmed mean across five biological replicates and six sampling times followed by trait-wise z-score standardisation.

Key microbial populations in the biodegradable plastics

We investigated bioplastic biodegradation in more detail by analysing 227 medium to high quality MAGs (79.3% ± 2.1% complete, 2.8% ± 0.3% redundant) that recruited ≥ 0.5% of the reads in the CA, PBS, and PHB *in situ* and *in vitro* metagenomes and metatranscriptomes, or that were significantly more abundant in these compared to the inert materials (linear regression, log2FC ≥ 3.0, adjusted $P < 0.05$) (**Table S2**). Genes involved in the initial hydrolysis of CA, PBS, and PHB were detected in 14.5%, 18.9%, and 61.7% of the MAGs, respectively, and 19.8% encoded the genes for two or more bioplastics (**Fig. 4a**). Most MAGs with bioplastic-degrading genes belonged to *Alpha-* and *Gammaproteobacteria*, *Actinomycetota*, *Bacteroidota*, and *Myxococcota* (**Fig. 4b**).

The *in vitro* metatranscriptomes enabled us to probe the activity of specific genes and identify microbial populations that are likely involved in bioplastic biodegradation. Given that bioplastic was the only carbon source in the *in vitro* experiments, the metatranscriptomic signal of key bioplastic-degrading genes provides strong indication of microbial populations that are actively participating in the biodegradation of these materials. Metatranscriptomic activity was observed for 36.3%, 16.3% and 42.9% of the MAGs carrying the genes for CA, PBS, and PHB hydrolysis, respectively (**Fig. 4c, Table S2**). Many MAGs belonged to genera

that were abundant in the biodegraded plastics according to the analysis of single-copy marker genes (**Fig. 2c**). Metatranscriptomic activity for PBS was detected in abundant MAGs assigned to *Microbacterium* (*Actinomycetota*), *Acidovorax*, and *Hydrogenophaga* (both *Gammaproteobacteria*), as well as in less abundant *Alphaproteobacteria* and *Myxococcota* MAGs (**Fig. 4c, Fig. 5**). In addition to PBS, the *Acidovorax* and *Hydrogenophaga* MAGs also had active genes for PHB degradation. The two *Nannocystaceae* (*Myxococcota*) MAGs and one *Simiduia* (*Gammaproteobacteria*) MAG encoded the potential to degrade the three bioplastics, but metatranscriptomic activity for PBS was not detected. Other MAGs with metatranscriptomic activity for CA included members of the *Bacteroidota* and *Verrucomicrobiota*, and MAGs with activity for PHB were diverse.

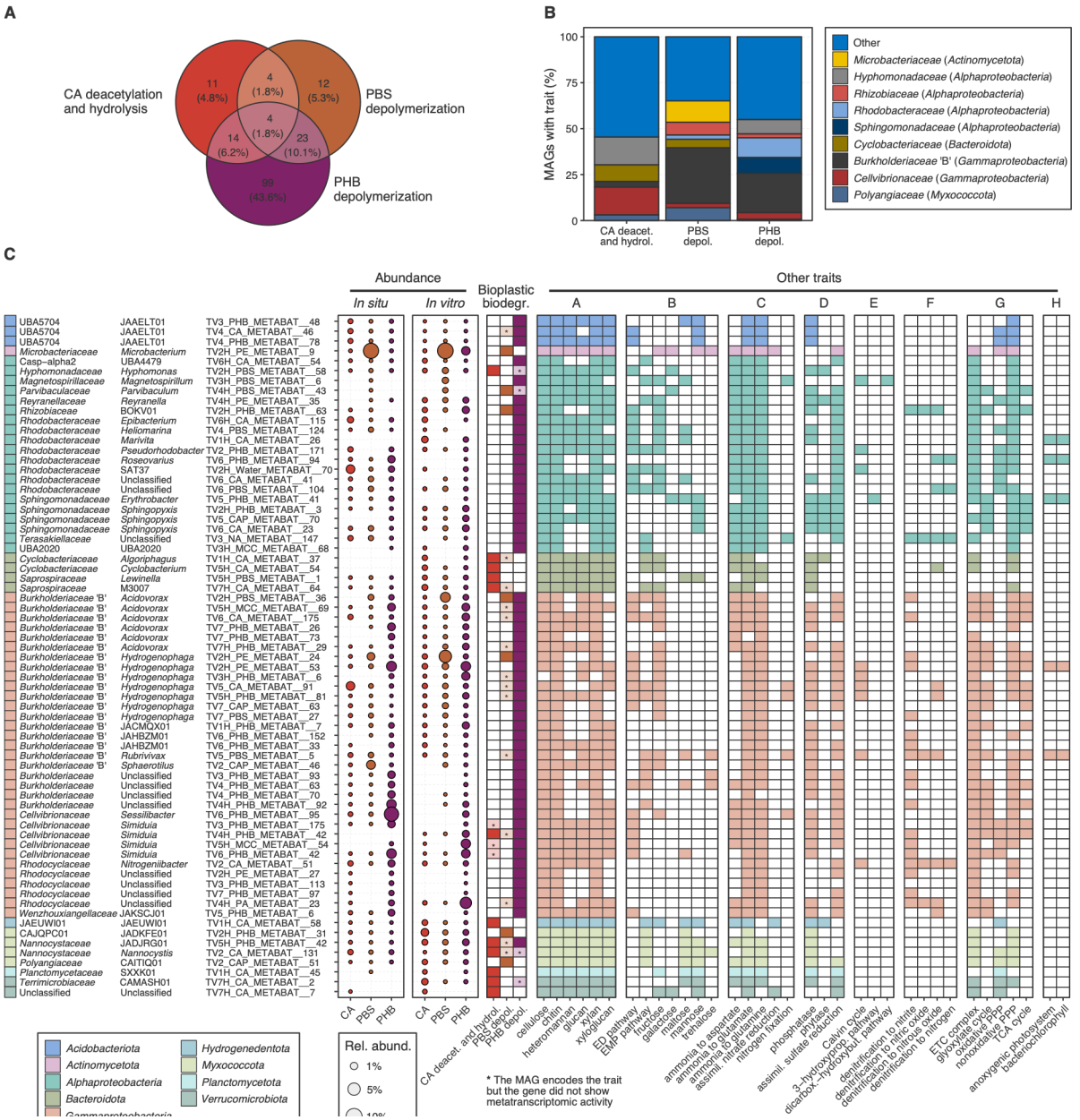

Figure 4 (see caption in next page).

Figure 4 (previous page). Microbial populations from the Baltic Sea with putative function in bioplastic biodegradation. Metagenome-assembled genomes (MAGs) (n = 227) with ≥ 0.5% relative abundance in the CA, PBS, and PHB *in situ* and *in vitro* metagenomes and metatranscriptomes, or that were significantly more abundant in these compared to the inert materials (PA, PE, and glass) according to linear regression (log2FC ≥ 3.0, adjusted $P < 0.05$). **a)** Distribution of putative plastic-degrading genes across the 227 MAGs and **b)** and their family-level taxonomic classification. **c)** Detailed information on a subset of MAGs (n = 69) which had plastic genes with activity in the *in vitro* metatranscriptomes. A: Complex carbohydrate depolymerization; B: Degradation of carbohydrates, sugar acids and proteins; C: Assimilation of N compounds; D: Assimilation of P and S compounds; E: CO_2 fixation; F: Anaerobic respiration; G: Aerobic respiration; H: Photosynthesis.

Metabolic reconstruction suggested that the populations with a putative function on CA, PBS, and PHB degradation comprised mostly aerobic heterotrophs with broad carbohydrate-degrading capabilities, including the breakdown of cellulose, chitin, heteromannan, glucan, xylan and xyloglucan (**Fig. 4c**, **Fig. 5, Table S2**). Several *Alpha-* and *Gammaproteobacteria* MAGs also encoded the potential for anaerobic respiration via complete and truncated denitrification (to nitrite, nitric oxide, or nitrous oxide), CO_2 fixation (mostly via the Calvin cycle), anoxygenic photosynthesis, and nitrogen fixation.

Discussion

Our combined experimental approach, which included multi-seasonal *in situ* and *in vitro* metagenomic and metatranscriptomic data, enabled a detailed characterisation of the biodegradation of different bioplastics in the Baltic Sea. We observed variable biodegradation rates across materials, seasons, and experimental settings. CA, PBS, and PHB degraded 7–28% after 97 weeks *in situ* and 27–56% after four weeks *in vitro*, whereas CAP, PA, and PE had low to negligible biodegradation. In line with our hypothesis, the structure of mature (> 1 month) microbial communities differed between all the bioplastics in both taxonomic and functional spaces. However, we observed more pronounced differences between the biodegraded and non-biodedegraded plastics than within each of these groups, indicating that community development is strongly influenced by the biodegradability of the materials, as previously observed [18, 26, 71]. Community structure changed gradually from the biodegraded plastics (CA, PBS, and PHB) to the slowly-degrading plastic (CAP) and the inert materials (PA, PE, and glass), suggesting that community development on biodegradable plastics is more dynamic than on conventional plastics, in which communities are considered mature after around one month [19]. The clustering of PA and PE with glass agrees with other studies and suggests that non-biodegradable plastics act mainly as a substrate for biofilm development in marine environments, having little effect on community composition [19, 22, 26, 30, 71]. Overall, our results show that distinct biodegradable plastics can support taxonomically and functionally convergent microbial communities, which we refer to as the *bioplastisphere*.

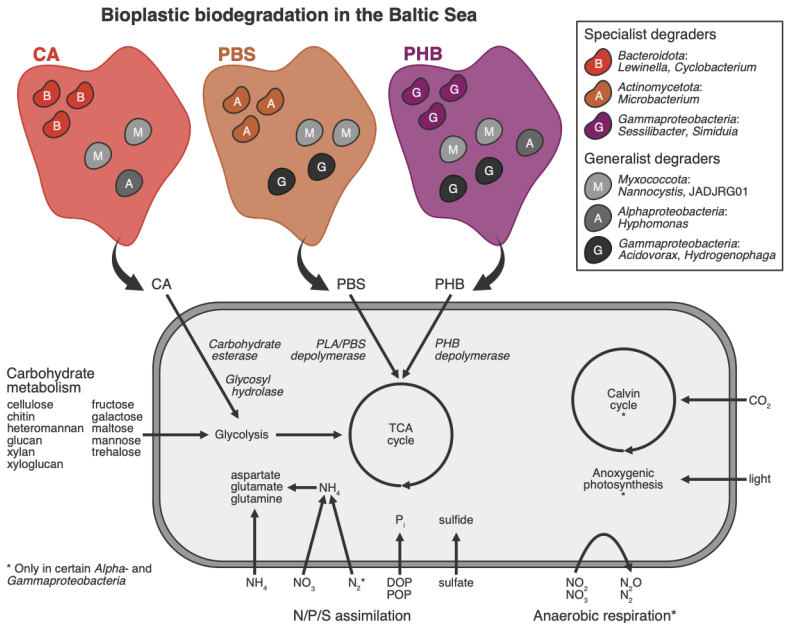

Figure 5. Conceptual illustration of bioplastic biodegradation in the Baltic Sea. Examples of abundant populations on CA, PBS, and PHB with metatranscriptomic activity of plastic-degrading genes, including populations of specialist and generalist degraders (active on one or many substrates, respectively). The metabolic diagram represents the aggregated metabolism of different populations with putative function on bioplastic biodegradation.

The communities on CAP, which degraded albeit slowly, shared similarities to the communities on both the biodegraded and non-biodegraded plastics. In particular, the functional composition of the communities on CAP was similar to the bioplastisphere communities, suggesting that the biodegradation potential of CAP is comparable to the other materials, despite much slower biodegration rates. In addition to environmental drivers, the biodegradation of cellulose derivatives depends on the degree of substitution and size of the ester group [72]. The high degradation of PBS observed in our study is in contrast with previous investigations in marine and freshwater environments [25], and only the biodegradation of PBS with low molecular weight has been previsouly measured in marine environments [73]. The higher *in vitro* biodegradation rates compared to *in situ* might be attributed to experimental differences in material geometry (< 0.3 mm particles were used *in vitro* and 3 mm-thick sheets *in situ*), given that smaller plastic particles are generally easier to degrade [26, 74]. The addition of nitrogen and phosphorus in the *in vitro* incubations might have also contributed to the higher biodegradation rates. We observed variable *in vitro* biodegradation rates for each material between the different sampling times. Given that the *in vitro* experiments were done under controlled environmental settings, this suggests that the biodegradation potential of the Baltic Sea bioplastisphere fluctuates between seasons and years. Seasonal variation in biodegradation potential [26] and microbial community structure [21, 27] has been observed in previous studies. The highest biodegradation of PHB was observed in winter and coincided with a high relative abundance of *Gammaproteobacteria*, which are known to produce and degrade PHB in cold environments

407 [75, 76]. The opportunistic behaviour of *Gammaproteobacteria* is a well-known phenomenon
408 in decaying phytoplankton blooms and other natural pulse-like sources of dissolved organic
409 matter [77, 78]. Altogether, our results suggest that the effects of environmental conditions,
410 material geometry, and inoculum composition should be considered when assessing marine
411 bioplastic biodegradation.

412 Our genome-resolved analysis evidenced a widespread potential for CA, PBS, and PHB
413 degradation across the bioplastisphere independently of substrate, with many abundant
414 populations harbouring the potential to degrade multiple bioplastics. Importantly, the
415 metatranscriptomic activity of plastic-degrading genes provided strong indication of
416 microbial populations that can drive bioplastic biodegradation in the Baltic Sea. Populations
417 with active plastic-degrading were generally very abundant on the biodegraded plastics,
418 whereas the opposite is usually observed for conventional plastics [19]. Populations with
419 active plastic-degrading genes included common members of the marine plastisphere such as
420 *Hyphomonas* (*Alphaproteobacteria*), *Sessilibacter*, and *Simiduia* (both
421 *Gammaproteobacteria*) [22, 26, 28, 30], but also typically terrestrial taxa such as
422 *Microbacterium* (*Actinomycetota*), *Acidovorax,* and *Hydrogenophaga* (both
423 *Gammaproteobacteria*) that are generally common in coastal waters and estuaries [79–81].
424 Our results are therefore likely to be relevant to other coastal and estuarine systems, but
425 differences are expected considering that biogeographical and environmental factors are
426 known to influence the composition of the plastisphere [21, 22, 27–29].

427 Metabolic reconstruction revealed that the active members of the bioplastisphere are
428 comprised mainly of aerobic and facultative anaerobic heterotrophs that encode the potential
429 to degrade complex carbohydrates and polymers. The bioplastisphere populations were also
430 enriched in anaerobic and nitrogen cycle traits compared to the non-biodegradable plastics.
431 Our results indicate that nitrogen fixation might be an important strategy to counterbalance
432 nitrogen deficiency when growing on the carbon-rich bioplastic materials [16, 24, 82].
433 Together with the increased capacity for anaerobic respiration via denitrification, these
434 results also suggest that biofilm development on biodegradable plastics promotes low-oxygen
435 microhabitats that favour facultative anaerobes [16, 24]. In addition, our results indicate that
436 most bioplastisphere denitrifier populations have truncated pathways, as has been observed
437 for other marine as well as terrestrial ecosystems [83, 84], and included populations with
438 putative truncated pathways leading to the release of nitrous oxide. Overall, our study
439 suggests that the bioplastisphere populations encoding the potential to degrade bioplastics
440 are microbial generalists adapted to a range of oxygen, carbon, and nutrient availabilities,
441 with diverse couplings to the overall marine carbon and nitrogen cycles.

442 Our study indicates that bioplastic biodegradability might be on itself a stronger driver of
443 microbial community composition than specific physicochemical properties of the plastic
444 materials, with the carbon derived from the breakdown of different bioplastics maintaining
445 a common bioplastisphere. We have shown that large bioplastic fragments, equivalent to
446 common items such as beverage bottles and disposable cuttlery, degrade in brackish seawater
447 at rates that are much slower than those required by current industrial standards regulating

bioplastic labelling. There needs to be a greater emphasis on developing more robust industrial regulations that consider more broadly the issue of mismanaged bioplastic waste that ends up in the marine environment, where they might persist for years or decades causing prolonged environmental harm. Although the search for marine biodegradable plastics and further characterisation of the bioplastisphere is an important way forward to mitigate plastic pollution, attention should be put in ensuring proper disposal of plastic waste and reducing plastic production at the source, which would also alleviate energy demands and greenhouse gas emissions.

Author contributions

ISP: Formal analysis, Software, Visualization, Writing – original draft, Writing – review & editing. **EE-R:** Conceptualization, Funding acquisition, Investigation, Writing – original draft, Writing – review & editing. **PN:** Investigation, Writing – review & editing. **DNT:** Conceptualization, Funding acquisition, Investigation, Writing – review & editing. **HK:** Conceptualization, Funding acquisition, Investigation, Project administration, Writing – review & editing.

Conflicts of interest

The authors declare no conflict of interest.

Acknowledgements

We thank Anna Kangas, Anni Jylhä-Vuorio, and Elisa Sillförs for help with the experimental work; Murat Eren, Iva Veseli, Florian Trigodet, Tom Delmont, and Laura Cappelatti for interesting discussions and ideas; and Minna Maunula and the students of the Microbiologist's Toolkit course (Autumn 2025, University of Helsinki) for insightful feedback on an earlier version of the manuscript. We acknowledge the DNA Sequencing and Genomics Laboratory (Institute of Biotechnology, University of Helsinki) for sequencing and the CSC–IT Centre for Finland for the computing infrastructure. No LLM/genAI tools were used in this study.

Study funding

This study was supported by the Research Council of Finland (grant number 332174).

Data availability

The metagenomic and metatranscriptomic data for this study have been deposited in the European Nucleotide Archive (ENA) at EMBL-EBI under the accession number PRJEB98035 (ebi.ac.uk/ena/browser/view/PRJEB98035).

Supplementary material

Pessi_et_al_2025_Suppl_Figs.docx: Supplementary figures S1–S8.

Pessi_et_al_2025_Suppl_Tables.xlsx: Supplementary tables S1–S2.

References

1. Jambeck JR et al. Plastic waste inputs from land into the ocean. *Science* 2015;**347**:768–771. https://doi.org/10.1126/science.1260352
2. Lebreton LCM et al. River plastic emissions to the world's oceans. *Nat Commun* 2017;**8**:15611. https://doi.org/10.1038/ncomms15611
3. Meijer LJJ et al. More than 1000 rivers account for 80% of global riverine plastic emissions into the ocean. *Sci Adv* 2021;**7**:eaaz5803. https://doi.org/10.1126/sciadv.aaz5803
4. Andrady AL. Persistence of plastic litter in the oceans. In: Bergmann M, Gutow L, Klages M (eds), Marine anthropogenic litter. Cham: Springer International Publishing, 2015, 57–72.
5. Napper IE, Thompson RC. Plastic debris in the marine environment: History and future challenges. *Global Chall* 2020;**4**:1900081. https://doi.org/10.1002/gch2.201900081
6. Lebreton L, Andrady A. Future scenarios of global plastic waste generation and disposal. *Palgrave Commun* 2019;**5**:6. https://doi.org/10.1057/s41599-018-0212-7
7. Int-Veen I et al. Positively buoyant but sinking: polymer identification and composition of marine litter at the seafloor of the North Sea and Baltic Sea. *Mar Pollut Bull* 2021;**172**:112876. https://doi.org/10.1016/j.marpolbul.2021.112876
8. Jylhä-Vuorio A et al. Incorporation of plastic debris into the nests of great cormorants (*Phalacrocorax carbo sinensis*) in the Gulf of Finland. *Mar Pollut Bull* 2024;**208**:116934. https://doi.org/10.1016/j.marpolbul.2024.116934
9. European Commission. Biodegradability of plastics in the open environment. European Commission, 2020. https://data.europa.eu/doi/10.2777/690248
10. European Commission. Requirements for packaging recoverable through composting and biodegradation: test scheme and evaluation criteria for the final acceptance of packaging. European Commission, 2000. http://data.europa.eu/eli/dec/2001/524.
11. Venâncio C, Lopes I, Oliveira M. Bioplastics: Known effects and potential consequences to marine and estuarine ecosystem services. *Chemosphere* 2022;**309**:136810. https://doi.org/10.1016/j.chemosphere.2022.136810
12. Lott C et al. Half-life of biodegradable plastics in the marine environment depends on material, habitat, and climate zone. *Front Mar Sci* 2021;**8**:662074. https://doi.org/10.3389/fmars.2021.662074

515 13. Choe S et al. Bridging three gaps in biodegradable plastics: misconceptions and truths
516 about biodegradation. *Front Chem* 2021;**9**:671750.
517 https://doi.org/10.3389/fchem.2021.671750

518 14. Carpenter EJ et al. Polystyrene spherules in coastal waters. *Science* 1972;**178**:749–750.
519 https://doi.org/10.1126/science.178.4062.749

520 15. Zettler ER, Mincer TJ, Amaral-Zettler LA. Life in the "plastisphere": microbial
521 communities on plastic marine debris. *Environ Sci Technol* 2013;**47**:7137–7146.
522 https://doi.org/10.1021/es401288x

523 16. Amaral-Zettler LA, Zettler ER, Mincer TJ. Ecology of the plastisphere. *Nat Rev Microbiol*
524 2020;**18**:139–151. https://doi.org/10.1038/s41579-019-0308-0

525 17. Lobelle D, Cunliffe M. Early microbial biofilm formation on marine plastic debris. *Mar*
526 *Pollut Bull* 2011;**62**:197–200. https://doi.org/10.1016/j.marpolbul.2010.10.013

527 18. Dussud C et al. Colonization of non-biodegradable and biodegradable plastics by marine
528 microorganisms. *Front Microbiol* 2018;**9**:1571. https://doi.org/10.3389/fmicb.2018.01571

529 19. Wright RJ et al. Marine plastic debris: a new surface for microbial colonization. *Environ*
530 *Sci Technol* 2020;**54**:11657–11672. https://doi.org/10.1021/acs.est.0c02305

531 20. Cheng J et al. Relative influence of plastic debris size and shape, chemical composition
532 and phytoplankton-bacteria interactions in driving seawater plastisphere abundance,
533 diversity and activity. *Front Microbiol* 2021;**11**:610231.
534 https://doi.org/10.3389/fmicb.2020.610231

535 21. Oberbeckmann S et al. Spatial and seasonal variation in diversity and structure of
536 microbial biofilms on marine plastics in Northern European waters. *FEMS Microbiol*
537 *Ecol* 2014;**90**:478–492. https://doi.org/10.1111/1574-6941.12409

538 22. Oberbeckmann S, Labrenz M. Marine microbial assemblages on microplastics: diversity,
539 adaptation, and role in degradation. *Annu Rev Mar Sci* 2020;**12**:209–232.
540 https://doi.org/10.1146/annurev-marine-010419-010633

541 23. Wright RJ, Langille MGI, Walker TR. Food or just a free ride? A meta-analysis reveals
542 the global diversity of the Plastisphere. *The ISME Journal* 2021;**15**:789–806.
543 https://doi.org/10.1038/s41396-020-00814-9

544 24. Fortin SG et al. Microplastic biofilms as potential hotspots for plastic biodegradation and
545 nitrogen cycling: a metagenomic perspective. *FEMS Microbiol Ecol* 2025;**101**:fiaf035.
546 https://doi.org/10.1093/femsec/fiaf035

547 25. Morohoshi T et al. Molecular characterization of the bacterial community in biofilms for
548 degradation of poly(3-hydroxybutyrate-*co*-3-hydroxyhexanoate) films in seawater.
549 *Microbes Environ* 2018;**33**:19–25. https://doi.org/10.1264/jsme2.ME17052

550 26. Eronen-Rasimus EL, Näkki PP, Kaartokallio HP. Degradation rates and bacterial
551 community compositions vary among commonly used bioplastic materials in a brackish

552 marine environment. *Environ Sci Technol* 2022;**56**:15760−15769.
553 https://doi.org/10.1021/acs.est.2c06280

554 27. Oberbeckmann S, Osborn AM, Duhaime MB. Microbes on a bottle: substrate, season and
555 geography influence community composition of microbes colonizing marine plastic debris.
556 *PLoS ONE* 2016;**11**:e0159289. https://doi.org/10.1371/journal.pone.0159289

557 28. Oberbeckmann S, Kreikemeyer B, Labrenz M. Environmental factors support the
558 formation of specific bacterial assemblages on microplastics. *Front Microbiol*
559 2018;**8**:2709. https://doi.org/10.3389/fmicb.2017.02709

560 29. Amaral-Zettler LA et al. The biogeography of the plastisphere: implications for policy.
561 *Frontiers Ecol Environ* 2015;**13**:541–546. https://doi.org/10.1890/150017

562 30. Rogers KL et al. Micro-by-micro interactions: how microorganisms influence the fate of
563 marine microplastics. *Limnol Oceanogr Lett* 2020;**5**:18–36.
564 https://doi.org/10.1002/lol2.10136

565 31. Pinnell LJ, Turner JW. Shotgun metagenomics reveals the benthic microbial community
566 response to plastic and bioplastic in a coastal marine environment. *Front Microbiol*
567 2019;**10**:1252. https://doi.org/10.3389/fmicb.2019.01252

568 32. Odobel C et al. Bacterial abundance, diversity and activity during long-term colonization
569 of non-biodegradable and biodegradable plastics in seawater. *Front Microbiol*
570 2021;**12**:734782. https://doi.org/10.3389/fmicb.2021.734782

571 33. Deroiné M et al. Natural degradation and biodegradation of poly(3-hydroxybutyrate-co-
572 3-hydroxyvalerate) in liquid and solid marine environments. *J Polym Environ*
573 2015;**23**:493–505. https://doi.org/10.1007/s10924-015-0736-5

574 34. Kirstein IV et al. Mature biofilm communities on synthetic polymers in seawater –
575 specific or general? *Mar Environ Res* 2018;**142**:147–154.
576 https://doi.org/10.1016/j.marenvres.2018.09.028

577 35. Kirstein IV et al. The plastisphere – uncovering tightly attached plastic "specific"
578 microorganisms. *PLoS ONE* 2019;**14**:e0215859.
579 https://doi.org/10.1371/journal.pone.0215859

580 36. Connors E et al. Changes in microbial community structure of bio-fouled polyolefins over
581 a year-long seawater incubation in Hawai'i. *Environ Microbiol Rep* 2024;**16**:e13283.
582 https://doi.org/10.1111/1758-2229.13283

583 37. Scott J et al. Systematic critical review of studies and methods assessing microbial
584 degradation of plastics in the marine environment: evidence base and recommendations.
585 *Sci Total Environ* 2025;**999**:180277. https://doi.org/10.1016/j.scitotenv.2025.180277

586 38. Agilent. MicroLab. v5.8, 2024. https://www.agilent.com/en/product/molecular-
587 spectroscopy/ftir-spectroscopy/ftir-software/microlab-ftir-software

588 39. ASTM. Standard test method for determining aerobic biodegradation of plastic materials
589 in the marine environment by a defined microbial consortium or natural sea water
590 inoculum. ASTM, 2017. https://store.astm.org/d6691-17.html

591 40. Viitamäki S et al. The activity and functions of soil microbial communities in the Finnish
592 sub-Arctic vary across vegetation types. *FEMS Microbiol Ecol* 2022;**98**:fiac079.
593 https://doi.org/10.1093/femsec/fiac079

594 41. Martin M. Cutadapt removes adapter sequences from high-throughput sequencing reads.
595 *EMBnet J* 2011;**17**:10. https://doi.org/10.14806/ej.17.1.200

596 42. Andrews S. FastQC: A quality control tool for high throughput sequence data. v0.12.1,
597 2019. http://www.bioinformatics.babraham.ac.uk/projects/fastqc

598 43. Ewels P et al. MultiQC: Summarize analysis results for multiple tools and samples in a
599 single report. *Bioinformatics* 2016;**32**:3047–3048.
600 https://doi.org/10.1093/bioinformatics/btw354

601 44. Menzel P, Ng KL, Krogh A. Fast and sensitive taxonomic classification for metagenomics
602 with Kaiju. *Nat Commun* 2016;**7**:11257. https://doi.org/10.1038/ncomms11257

603 45. Woodcroft BJ et al. Comprehensive taxonomic identification of microbial species in
604 metagenomic data using SingleM and Sandpiper. *Nat Biotechnol* 2025;**in press**.
605 https://doi.org/10.1038/s41587-025-02738-1

606 46. Parks DH et al. GTDB: an ongoing census of bacterial and archaeal diversity through a
607 phylogenetically consistent, rank normalized and complete genome-based taxonomy.
608 *Nucleic Acids Res* 2022;**50**:D785–D794. https://doi.org/10.1093/nar/gkab776

609 47. Eren AM et al. Community-led, integrated, reproducible multi-omics with anvi'o. *Nat*
610 *Microbiol* 2021;**6**:3–6. https://doi.org/10.1038/s41564-020-00834-3

611 48. Li D et al. MEGAHIT: an ultra-fast single-node solution for large and complex
612 metagenomics assembly via succinct de Bruijn graph. *Bioinformatics* 2015;**31**:1674–
613 1676. https://doi.org/10.1093/bioinformatics/btv033

614 49. Hyatt D et al. Prodigal: prokaryotic gene recognition and translation initiation site
615 identification. *BMC Bioinform* 2010;**11**:119. https://doi.org/10.1186/1471-2105-11-119

616 50. Lee MD. GToTree: a user-friendly workflow for phylogenomics. *Bioinformatics*
617 2019;**35**:4162–4164. https://doi.org/10.1093/bioinformatics/btz188

618 51. Eddy SR. Accelerated profile HMM searches. *PLoS Comput Biol* 2011;**7**:e1002195.
619 https://doi.org/10.1371/journal.pcbi.1002195

620 52. Buchfink B, Xie C, Huson DH. Fast and sensitive protein alignment using DIAMOND.
621 *Nat Methods* 2015;**12**:59–60. https://doi.org/10.1038/nmeth.3176

622 53. Langmead B, Salzberg SL. Fast gapped-read alignment with Bowtie 2. *Nat Methods*
623 2012;**9**:357–359. https://doi.org/10.1038/nmeth.1923

624 54. Li H et al. The Sequence Alignment/Map format and SAMtools. *Bioinformatics*
625 2009;**25**:2078–2079. https://doi.org/10.1093/bioinformatics/btp352

626 55. Kang DD et al. MetaBAT 2: An adaptive binning algorithm for robust and efficient
627 genome reconstruction from metagenome assemblies. *PeerJ* 2019;**7**:e7359.
628 https://doi.org/10.7717/peerj.7359

629 56. Jain C et al. High throughput ANI analysis of 90K prokaryotic genomes reveals clear
630 species boundaries. *Nat Commun* 2018;**9**:5114. https://doi.org/10.1038/s41467-018-
631 07641-9

632 57. Olm MR et al. dRep: a tool for fast and accurate genomic comparisons that enables
633 improved genome recovery from metagenomes through de-replication. *ISME J*
634 2017;**11**:2864–2868. https://doi.org/10.1038/ismej.2017.126

635 58. Pessi IS, Rutanen A, Hultman J. Metagenome-assembled genomes from mineral tundra
636 soils in Rásttigáisá, northern Norway. *Access Microbiology* 2024;**6**:000655.
637 https://doi.org/10.1099/acmi.0.000655.v3

638 59. Chaumeil P-A et al. GTDB-Tk v2: memory friendly classification with the genome
639 taxonomy database. *Bioinformatics* 2022;**38**:5315–5316.
640 https://doi.org/10.1093/bioinformatics/btac672

641 60. Aroney STN et al. CoverM: read alignment statistics for metagenomics. *Bioinformatics*
642 2025;**41**:btaf147. https://doi.org/10.1093/bioinformatics/btaf147

643 61. Karaoz U, Brodie EL. microTrait: a toolset for a trait-based representation of microbial
644 genomes. *Front Bioinform* 2022;**2**:918853. https://doi.org/10.3389/fbinf.2022.918853

645 62. Drula E et al. The carbohydrate-active enzyme database: functions and literature.
646 *Nucleic Acids Res* 2022;**50**:D571–D577. https://doi.org/10.1093/nar/gkab1045

647 63. Gambarini V et al. PlasticDB: a database of microorganisms and proteins linked to plastic
648 biodegradation. *Database* 2022;**2022**:baac008. https://doi.org/10.1093/database/baac008

649 64. R Core Team. R: a language and environment for statistical computing. v4.3.3, 2024.
650 https://www.r-project.org

651 65. Lenth RV. emmeans: estimated marginal means, aka least-squares means. v1.10.6, 2024.
652 https://CRAN.R-project.org/package=emmeans

653 66. Hothorn T, Bretz F, Westfall P. multcomp: simultaneous inference in general parametric
654 models. v1.4.26, 2024. https://CRAN.R-project.org/package=multcomp

655 67. Oksanen J et al. vegan: community ecology package. v2.7.1, 2025. https://cran.r-
656 project.org/package=vegan

657 68. Mallick H et al. Multivariable association discovery in population-scale meta-omics
658 studies. *PLoS Comput Biol* 2021;**17**:e1009442.
659 https://doi.org/10.1371/journal.pcbi.1009442

69. Bryant JA et al. Diversity and activity of communities inhabiting plastic debris in the North Pacific Gyre. *mSystems* 2016;**1**:e00024-16. https://doi.org/10.1128/msystems.00024-16

70. Mayumi D et al. Identification and characterization of novel poly(dl-lactic acid) depolymerases from metagenome. *Appl Microbiol Biotechnol* 2008;**79**:743–750. https://doi.org/10.1007/s00253-008-1477-3

71. Ridley RS et al. Potential routes of plastics biotransformation involving novel plastizymes revealed by global multi-omic analysis of plastic associated microbes. *Sci Rep* 2024;**14**:8798. https://doi.org/10.1038/s41598-024-59279-x

72. Erdal NB, Hakkarainen M. Degradation of cellulose derivatives in laboratory, man-made, and natural environments. *Biomacromolecules* 2022;**23**:2713–2729. https://doi.org/10.1021/acs.biomac.2c00336

73. Tachibana Y et al. Can poly(butylene succinate) degrade in seawater? *Chemosphere* 2025;**374**:144203. https://doi.org/10.1016/j.chemosphere.2025.144203

74. Beiras R, López-Ibáñez S. A practical tool for the assessment of polymer biodegradability in marine environments guides the development of truly biodegradable plastics. *Polymers* 2023;**15**:974. https://doi.org/10.3390/polym15040974

75. Verlinden RAJ et al. Bacterial synthesis of biodegradable polyhydroxyalkanoates. *J Appl Microbiol* 2007;**102**:1437–1449. https://doi.org/10.1111/j.1365-2672.2007.03335.x

76. Eronen-Rasimus E et al. Sea-ice bacteria *Halomonas* sp. strain 363 and *Paracoccus* sp. strain 392 produce multiple types of poly-3-hydroxyalkaonoic acid (PHA) storage polymers at low temperature. *Appl Environ Microbiol* 2021;**87**:e00929-21. https://doi.org/10.1128/AEM.00929-21

77. Eronen-Rasimus E et al. Bacterial community dynamics and activity in relation to dissolved organic matter availability during sea-ice formation in a mesocosm experiment. *MicrobiologyOpen* 2014;**3**:139–156. https://doi.org/10.1002/mbo3.157

78. Teeling H et al. Substrate-controlled succession of marine bacterioplankton populations induced by a phytoplankton bloom. *Science* 2012;**336**:608–611. https://doi.org/10.1126/science.1218344

79. Zeghal E et al. Environmental factors control microbial colonization of plastics in the North Sea. *Mar Pollut Bull* 2024;**208**:116964. https://doi.org/10.1016/j.marpolbul.2024.116964

80. Wang Z et al. *Acidovorax* PSJ13, a novel, efficient polyacrylamide-degrading bacterium by cleaving the main carbon chain skeleton without the production of acrylamide. *Biodegradation* 2023;**34**:581–595. https://doi.org/10.1007/s10532-023-10036-3

81. Hansen J et al. Effect of polymer type on the colonization of plastic pellets by marine bacteria. *FEMS Microbiol Lett* 2021;**368**:fnab026. https://doi.org/10.1093/femsle/fnab026

697 82. Du Y et al. A review on marine plastisphere: biodiversity, formation, and role in
698 degradation. *Comput Struct Biotechnol J* 2022;**20**:975–988.
699 https://doi.org/10.1016/j.csbj.2022.02.008

700 83. Rasigraf O et al. Microbial community composition and functional potential in Bothnian
701 Sea sediments is linked to Fe and S dynamics and the quality of organic matter. *Limnol*
702 *Oceanogr* 2020;**65**:S113–S133. https://doi.org/10.1002/lno.11371

703 84. Pessi IS et al. In-depth characterization of denitrifier communities across different soil
704 ecosystems in the tundra. *Environ Microbiome* 2022;**17**:30.
705 https://doi.org/10.1186/s40793-022-00424-2